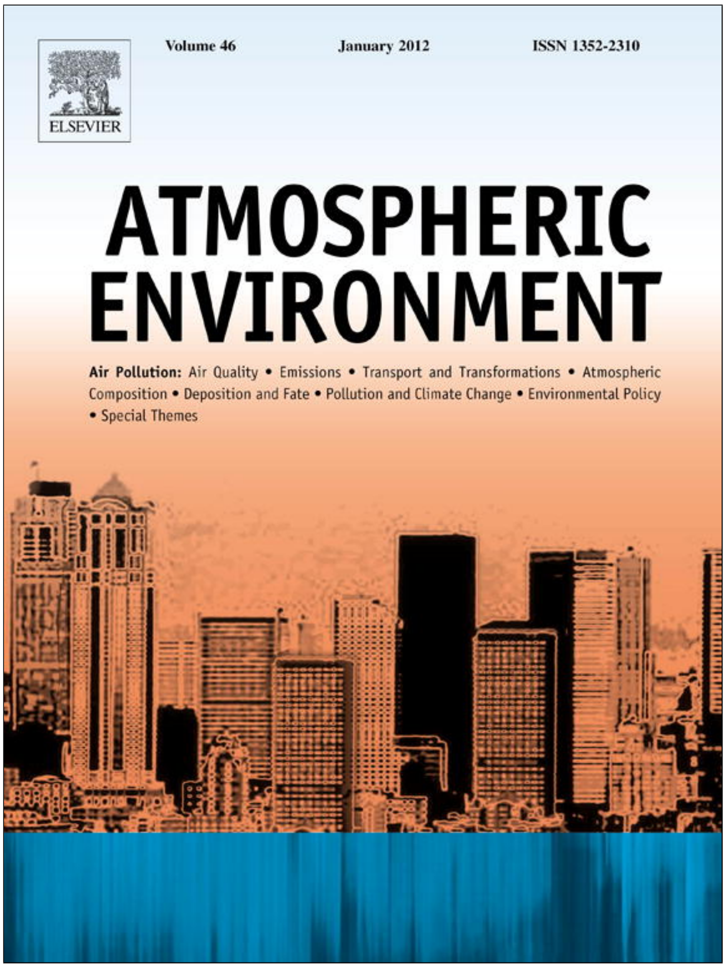
Volume 46
January 2012
ISSN 1352-2310
ELSEVIER
ATMOSPHERIC ENVIRONMENT
Air Pollution: Air Quality • Emissions • Transport and Transformations • Atmospheric Composition • Deposition and Fate • Pollution and Climate Change • Environmental Policy • Special Themes

Atmospheric Environment 69 (2013) 334–344

Contents lists available at SciVerse ScienceDirect

Atmospheric Environment

journal homepage: www.elsevier.com/locate/atmosenv

Long term climatology of particulate matter and associated microphysical and optical properties over Dibrugarh, North-East India and inter-comparison with SPRINTARS simulations

Binita Pathak [a], Pradip Kumar Bhuyan [a,*], Jhuma Biswas [a], Toshihiko Takemura [b]

[a] Centre for Atmospheric Studies, Dibrugarh University, Dibrugarh 786 004, India
[b] Research Institute for Applied Mechanics, Kyushu University, 6-1Kasuga-koen, Kasuga, Fukuoka 816-8580, Japan

HIGHLIGHTS

- ► The long term climatology indicates $PM_{2.5}$ is the principal contributor to the PM_{10} over Dibrugarh, North-East India.
- ► Maximum PM concentrations are positively correlated with fire counts over NE India and negatively correlated with rainfall.
- ► A slow decreasing trend in the PMs and BC concentrations has been observed during the study period.
- ► The SPRINTARS model underestimates the measured concentrations of PMs and BC except in pre-monsoon season.

ARTICLE INFO

Article history:
Received 24 May 2012
Received in revised form
24 December 2012
Accepted 27 December 2012

Keywords:
Aerosols
PM_{10}
$PM_{2.5}$
QCM
SPRINTARS

ABSTRACT

The long term climatology of PM_{10} and $PM_{2.5}$ concentrations for the five year period from June 2007–March 2012 is studied using measurements made with a Quartz Crystal Microbalance Impactor over Dibrugarh, North-East India. The PM_{10} and $PM_{2.5}$ exhibit similar seasonal variability with maximum concentration in winter and minimum in monsoon seasons. The PM_{10} concentration is mainly attributed to $PM_{2.5}$ with minimal contribution from $PM_{10-2.5}$. The long term monthly mean PM_{10} and $PM_{2.5}$ concentrations shows maximum value in late winter and early pre-monsoon. This temporal variability is positively correlated with the MODIS retrieved fire counts associated mostly with the biomass burning activities and negatively correlated with rainfall. PM_{10} and $PM_{2.5}$ gradually increased from 2007 to 2010 and decreased thereafter. An overall slow decreasing trend in PM_{10} and $PM_{2.5}$ concentrations together with black carbon (BC) concentrations has been observed. The examination of microphysical and optical properties also reveals the dominance of $PM_{2.5}$ aerosols. Higher percentage contributions of BC to both PM_{10} and $PM_{2.5}$ are observed in post-monsoon season followed by winter. The inter-comparison of measured PM and BC concentrations with SPRINTARS simulation reveals that model underestimates the measurements except in pre-monsoon. The discrepancy might have arisen due to the topography of the location and inadequate emission inventory for the climate zone.

1. Introduction

Among the many pollutants, particulate matter (PM) has emerged as the most critical pollutant in almost all urban areas of the globe and its impacts on human health and ecology are the largest. The major anthropogenic sectors contributing to coarser fraction of PM i.e., PM_{10} are traffic, industry, agriculture and forestry, households, construction, quarrying and mining, cement plants and ceramic industries, fossil fuel power plants etc., while natural sources include the sea spray, soil resuspension, volcanic eruption, biological particles and debris etc. Carbonaceous and secondary species like sulphate, nitrate and ammonium are the major contributors of the fine fraction of PM i.e., $PM_{2.5}$ (Ye et al., 2003) in the regions intensively influenced by human activity. Due to wide distribution of sources the PM concentrations exhibit high degree of spatio-temporal variability in their physico-chemical and optical properties at short scales. As a result these aerosols have a wide range of direct and indirect influence on the environment, human health and climate (Forster et al., 2007). The respirable fractions PM_{10} and $PM_{2.5}$ have direct health

---

* Corresponding author. Tel.: +91 3732370224.
E-mail addresses: Pathak.binita8@gmail.com (B. Pathak), Bhuyan@dibru.ac.in, pkbhuyan@gmail.com (P.K. Bhuyan), Jhumabiswasdu@gmail.com (J. Biswas), toshi@riam.kyushu-u.ac.jp (T. Takemura).

1352-2310/$ – see front matter © 2013 Elsevier Ltd. All rights reserved.
http://dx.doi.org/10.1016/j.atmosenv.2012.12.032

consequences as they can penetrate deeper into the human respiratory systems. The $PM_{2.5}$ particles have the largest effect on short wave radiative transfer and contribute significantly to haze formation and visibility reduction. The study of the physical and optical parameters of the PM is, therefore, essential for a better understanding of their role in the atmospheric processes especially near the ground. The measurement of optical properties of PM, including extinction, scattering and absorption in the ultra violet, visible and infra-red spectral range provides a means of inferring atmospheric particle burden. In addition the mass concentration and mass size distribution of aerosols near the surface are vital inputs in aerosol models for estimation of radiative forcing, environmental effects and air quality.

Short term extensive measurement of surface aerosol concentration over India was made during ISRO GBP land campaign-I (1st–28th February 2004) and campaign-II (1st–31st December 2004) over south India and Indo-Gangetic plains respectively. During campaign-I Moorthy et al. (2005) have identified the hot-spots of aerosol concentration (>60 μg m^{-3}) around coastal, industrialized and urban areas of south India. Over the Indo-Gangetic plains very high concentration (260–300 μg m^{-3}) of aerosols was observed mainly over the three locations Kharagpur (22.52°N, 87.52°E), Allahabad (25.45°N, 81.85°E) and Kanpur (26.43°N, 80.33°E) (Moorthy et al., 2008). Apart from these campaigns measurements of surface aerosol concentration have been reported from other locations of India, e.g., by Latha and Badarinath (2005) over Hyderabad, Pant et al. (2006) over Nainital (29.2°N, 79.3°E), Ganguly et al. (2006) over Ahmedabad, Pillai and Moorthy (2001) and Moorthy et al. (2007) over Trivandrum.

The earlier reports on aerosols from Dibrugarh focused on columnar aerosol properties (Gogoi et al., 2008, 2009a,b, 2011; Pathak et al., 2010, 2012). However, Pathak et al. (2010) and Gogoi et al. (2011) have utilized short term surface aerosol measurements with emphasis on aerosol radiative forcing (ARF) and association of columnar aerosols with near surface aerosols respectively. In the present work the characteristics and long term climatology of the PM_{10} and $PM_{2.5}$ concentrations and their association with the possible production mechanisms and local meteorology has been examined. As black carbon forms a major fraction of surface aerosols with immense impact on regional and global climate, its contribution to PM_{10} and $PM_{2.5}$ are also investigated together with the physico-optical parameters of interest. As the spatial coverage of surface aerosol measurements are sparse and satellite retrievals till date do not provide the aerosol concentrations near the surface, one has to rely on model simulation for characterization of highly heterogeneous aerosols in both regional and global scale. Comparison of measured data with model are also essential to test the validity of the model simulation and helps in assessment of the retrieval algorithm, conditions under which the model works satisfactorily and cases where further improvements are needed. Therefore, measured PM_{10}, $PM_{2.5}$ and BC concentrations are compared with SPRINTARS (Spectral Radiation-Transport Model for Aerosol Species) simulations.

2. The study location, sampling method and data analysis

2.1. Study location

The study location Dibrugarh (27.3°N, 94.6°E, 111 m amsl) (Fig. 1) is situated on the southern bank of river Brahmaputra in eastern Assam, the principal state in North-East (NE) India. The site is mostly vegetated, surrounded by the large number of tea plantations, rivers and rivulets. On the basis of columnar aerosol optical depth measurements made over this site for more than a decade

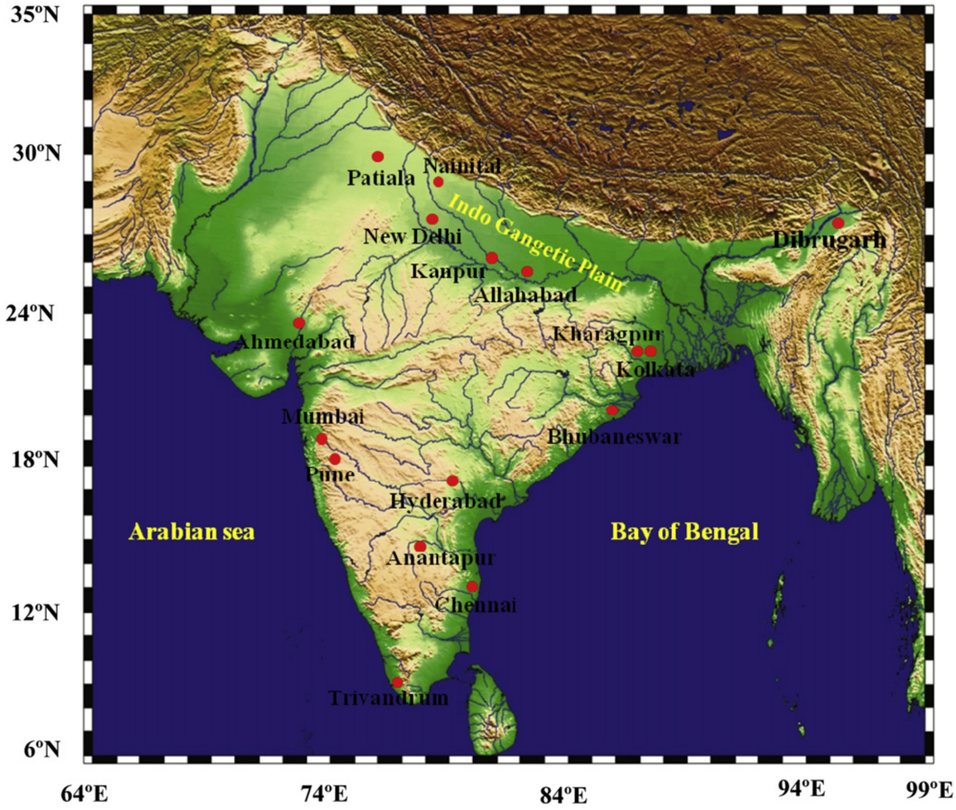

Fig. 1. Map of India showing the study location Dibrugarh (27.3°N, 94.6°E, 111 m amsl) and other locations of India cited in the paper (red dots). (For interpretation of the references to colour in this figure legend, the reader is referred to the web version of this article.)

Pathak et al. (2012) have considered this as a continental average i.e., rural in character but influenced by anthropogenic activities. In terms of human activity Dibrugarh is an urban location but with low population density and without heavy industrialization. Climatologically winter (December–February) is the driest season of the year at Dibrugarh and adjacent region with least rainfall (~4% of the annual), while monsoon (June–September) is the wettest season receiving maximum (63%) of annual rainfall with monthly rainy days varying between ~15 and 25 days. The relative humidity level is normally ≥60% while in monsoon it reaches ~80% and above. The minimum temperature ranges from ~8 °C in winter to ~20 °C in monsoon, while the range of maximum temperature is ~21 °C to ~36 °C in monsoon. Details of the study location and meteorology have been described by Gogoi et al. (2009a,b) and Pathak et al. (2012).

2.2. Sampling method and data analysis

Near surface aerosol mass and size distributions have been obtained using a Quartz Crystal Microbalance (QCM) Impactor (model PC-2, California Measurements Inc., USA). The QCM provides composite and size segregated mass concentration of aerosols at 10 different size ranges with a 50% efficiency (cutoff diameter are at >25: stage 1, 12.5, 6.25, 3.2, 1.6, 0.8, 0.4, 0.2, 0.1 and 0.05: stage 10) μm assuming a typical density of 2 g cm^{-3}, for continental aerosols. In terms of aerodynamic diameter at 50% efficiency the cutoff diameters for different stages of QCM are >35.37 (stage 1), 17.68, 9.05, 4.53, 2.26, 1.13, 0.57, 0.28, 0.14, 0.07 (stage 10) μm. The QCM samples air at a flow rate of 240 mL per minute. The measurements were restricted to RH ≤ 75% as quartz crystals are sensitive to high relative humidity. As such normally the observations were made at hourly intervals with sampling time duration of 5 min for each measurement from about 0700 h till 1900 h for 3–4 days in a week. The current data base comprises of 4141 samples in 873 days from 58 months for the period June 2007–March 2012. The measurement error for QCM remains within 15% (Moorthy et al., 2007).

During each measurement, the QCM provides the composite mass concentration (PM) which is the mass of aerosols for the above mentioned size ranges in unit volume of the ambient air and the mass concentration (m_{ci}) in each of its size bins $i = 1$–10. The composite PM concentration and m_{ci} are related as

$$\mathrm{PM} = \sum_{i=1}^{10} m_{ci} \qquad (1)$$

The composite PM concentration is further classified into PM_{10} (aerodynamic diameter ≤ 10 μm and QCM stages from 3 to 10) and $\mathrm{PM}_{2.5}$ (aerodynamic diameter ≤ 2.5 μm and QCM stages from 5 to 10) following Pillai and Moorthy (2001) as

$$\mathrm{PM}_{10} = \sum_{i=3}^{10} m_{ci} \qquad (2)$$

$$\mathrm{PM}_{2.5} = \sum_{i=5}^{10} m_{ci} \qquad (3)$$

It may be mentioned that the aerodynamic diameters of stages 3 and 5 of the QCM don't exactly match the upper cutoff diameters of PM_{10} and $\mathrm{PM}_{2.5}$. The QCM size segregated mass concentrations are further used to evaluate different microphysical and optical parameters viz. effective radius, mass mean radius, number-size distribution, size index and extinction coefficient following Pillai and Moorthy (2001) and Nair et al. (2008).

Black carbon mass concentration and absorption coefficient of aerosols (β_{abs}) at seven wavelength bands centred around 370, 470, 520, 590, 660, 880 and 950 nm are obtained from June 2008–March 2012 using a multichannel Aethalometer (model AE 31-ER from Magee Scientific). Details of the instrumentation, methodology and uncertainty are discussed elsewhere (e.g., Hansen et al., 1984; Babu et al., 2004; Nair et al., 2007; Pathak et al., 2010). The instrument is operated round the clock at a flow rate of 4 LPM and with a temporal resolution of 5 min. Observation at 880 nm wavelength is considered standard for BC measurement as BC is the principal absorber of light at this wavelength while other aerosol components have negligible absorption. The uncertainties in the Aethalometer technique arises from the multiple scattering effects in the filter tape and the shadowing effects (e.g., Weingartner et al., 2003; Arnott et al., 2005) and the corrections for these were done following Weingartner et al. (2003) and Nair et al. (2007).

2.3. SPRINTARS simulations

The SPRINTARS model developed by Takemura et al. (2009) is a global three-dimensional aerosol model, based on the atmospheric general circulation model. The model treats all of the main tropospheric aerosols, i.e., carbonaceous (black and organic carbons), sulphate, soil dust and sea salt and calculates a series of transport processes of emission, advection, diffusion, chemical reaction and deposition. The model is described in detail by Takemura et al. (2009 and references therein). The SPRINTARS has participated in the international global aerosol model intercomparison project, AeroCom (http://aerocom.met.no/) and its overall performance over the globe has been found to be satisfactory. Recently Goto et al. (2011a,b) have compared the measured BC, aerosol optical depth, Ångström exponent and single scattering albedo with SPRINTARS simulations over different locations in India. They have also estimated the impact of the discrepancy between measured and simulated optical properties in ARF.

3. Results and discussion

3.1. Temporal variation of PM concentrations

3.1.1. Seasonal variation of PM_{10}, $\mathrm{PM}_{2.5}$ and $\mathrm{PM}_{10-2.5}$

The seasonal distribution of climatological mean PM_{10}, $\mathrm{PM}_{2.5}$ and $\mathrm{PM}_{10-2.5}$ (PM_{10} minus $\mathrm{PM}_{2.5}$) concentrations averaged for the period June 2007–March 2012 is shown in Fig. 2 in the form of box plots. The highest seasonal mean concentrations of PM_{10} (57.2 ± 32.4 μg m^{-3}) and $\mathrm{PM}_{2.5}$ (51.9 ± 32.4 μg m^{-3}) are observed in winter season. Both PM_{10} and $\mathrm{PM}_{2.5}$ particle mass concentrations show similar seasonal variation with lowest values in monsoon (39.5 ± 19.6 and 32.0 ± 17.3 μg m^{-3} respectively). The PM_{10} and $\mathrm{PM}_{2.5}$ concentrations in pre-monsoon season are 53.2 ± 27.9 μg m^{-3} and 47.8 ± 27.3 μg m^{-3} and in post-monsoon season are 45.0 ± 24.3 μg m^{-3} and 37.3 ± 21.3 μg m^{-3} respectively. Thus, in terms of absolute concentrations PM_{10} may be nearly attributed to $\mathrm{PM}_{2.5}$. This is also evident from the seasonal $\mathrm{PM}_{2.5}/\mathrm{PM}_{10}$ ratios varying between ~81% in monsoon to 91% in winter and high seasonal correlation ($R^2 = \sim 0.97 - \sim 0.99$) between PM_{10} and $\mathrm{PM}_{2.5}$. Dominance of submicron aerosols have also been reported over Bay of Bengal (BoB) (Sinha et al., 2011 and references therein). This observation suggests that the source of both $\mathrm{PM}_{2.5}$ and PM_{10} are the same. The assessment of share of PM_{10} and $\mathrm{PM}_{2.5}$ to composite PM is significant from environmental and health perspective. The percentage share of PM_{10} to composite PM varies between ~89% in monsoon and ~94% in winter, while that of $\mathrm{PM}_{2.5}$ to composite PM lies within 72% in monsoon and 83% in

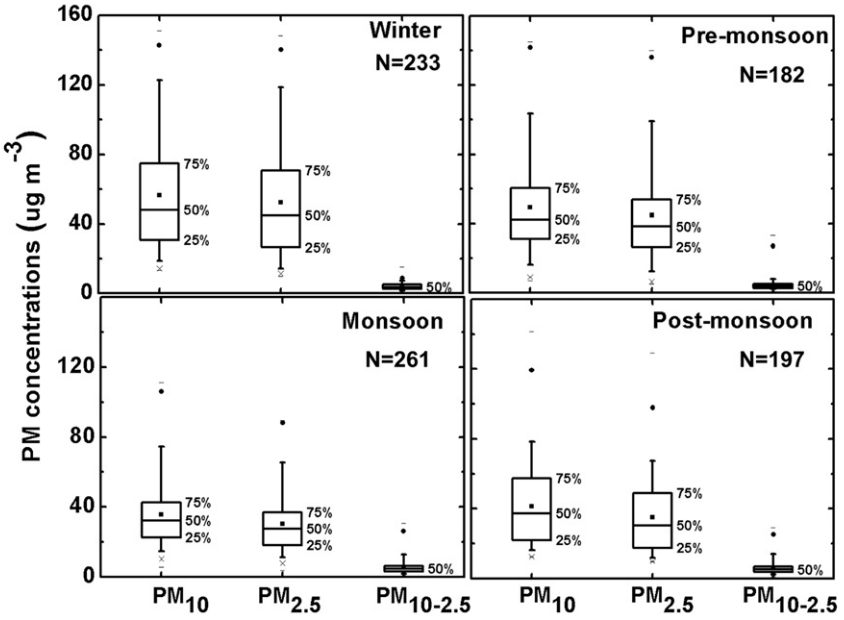

Fig. 2. Box plot showing the seasonal distribution of PM_{10}, $PM_{2.5}$ and $PM_{10-2.5}$ concentrations for the period June 2007–March 2012. The boxes represent 25th and 75th percentiles and the whiskers represent the 5th and 95th percentiles. The small box inside each box represents the mean value and the horizontal line represents the median value. *N* represents the number of days of observation.

winter. These large ratios are generally attributed to secondary particulate formation of species such as nitrate, sulphate, ammonium and organics (Song et al., 2009 and references therein). The secondary aerosols generated due to anthropogenic activities can exert a significant influence on the $PM_{2.5}$ concentration rather than on the $PM_{10-2.5}$ concentration. On the other hand the coarse fraction i.e., $PM_{10-2.5}$ concentration is least throughout the year with maximum in post-monsoon (7.6 ± 6.1 μg m^{-3}) and minimum in winter (5.2 ± 2.8 μg m^{-3}). The lowest abundance of coarse aerosols may be associated mainly with the vegetation cover over the location (Pathak et al., 2010) with insignificant contribution from dust aerosols.

The PM concentrations are driven by the dynamics of the atmosphere and the meteorological conditions. In winter the scanty rainfall associated with mostly clear sky and dry land conditions are highly favourable for generation and accumulation of continental aerosols both naturally and from anthropogenic activities. It is also associated with confinement of most of the particulates within the boundary layer, which comes down during this season. During pre-monsoon higher surface wind can lift and carry the soil derived dust aerosols from the dry Brahmaputra riverbed nearby to the site (Gogoi et al., 2008), which may contribute to PM_{10}. The effect of large scale forest fire in NE India region during pre-monsoon season (Kalita and Bhuyan, 2011) is prominent particularly in the month of March and April on near surface aerosol concentration. During monsoon, the wet removal processes lead to reduction in aerosol concentration in the atmosphere and hence PM concentrations reach to their minimum level. During post-monsoon reduction in rainfall favours generation of aerosols from both natural and anthropogenic sources. The transportation of fine aerosols from the oil wells, situated due east and north-east of the station and the national highway passing through the University campus contributes to fine ($PM_{2.5}$) aerosols throughout the year (Pathak et al., 2010). Trajectory clustering and concentration weighted trajectory analysis indicate that the potential sources across the west Asia and over the IGP mainly contribute to the seasonal maximum of PM concentrations over Dibrugarh during winter and pre-monsoon season adding to the local source effect. On the other hand, minor sources in the southwest to east of Dibrugarh modulate the aerosol properties during monsoon season, whereas moderate sources mostly localized to the south of Dibrugarh contribute to PMs during post-monsoon season (Gogoi et al., 2011).

Similar seasonal variability in PM_{10} and $PM_{2.5}$ concentrations with maximum during winter and minimum in monsoon season has been reported over a number of locations in India (Table 1) e.g., Hyderabad (Latha and Badarinath, 2005), Trivandrum (Pillai et al., 2002), Ahmedabad (Ganguly et al., 2006) and Anantapur (Balakrishnaiah et al., 2011). It is also obvious from Table 1 that values of seasonal PM concentrations reported by Pillai et al. (2002) over Trivandrum are comparable to the present measurements while these exceed the PM concentrations reported over Anantapur (Balakrishnaiah et al., 2011) and Hyderabad (Latha and Badarinath, 2005). The present measured values are less than those observed over megacities or urban locations like Kolkata, Delhi, Mumbai, Pune and highly polluted IGP or biomass burning active location Patiala.

3.1.2. Inter-annual variation of PM_{10} and $PM_{2.5}$

The annual variability in PM_{10} and $PM_{2.5}$ concentrations are shown in Fig. 3(a). The variability is same for both with annual high during January (2011), February (2009) or March (2008 and 2010). This may be attributed to reduced boundary layer height during winter months and maximum forest fires in the nearby regions during the pre-monsoon months. The annual minimum occurs during monsoon months which are associated with sufficient wet removal processes. There is an inter-annual variation in PM_{10} and $PM_{2.5}$ concentrations during winter and pre-monsoon of different years with maximum concentrations in 2009–2010 and minimum in 2010–2011. This difference is mainly confined to the winter and pre-monsoon seasons only while during monsoon the values are comparable in all the years. A linear regression through the data (Fig. 3(a)) indicates a slow decreasing trend in PM_{10} ($Y = -0.26X + 54.6$; $N = 58$; $F = 3.64$) and $PM_{2.5}$ ($Y = -0.21X + 46.3$; $N = 58$; $F = 2.54$). However, further examination of the monthly and

Table 1
PM_{10} and $PM_{2.5}$ concentrations measured at various locations in India including Dibrugarh.

Location	Time period	Seasons	Concentration (μg m^{-3})		References
			PM_{10}	$PM_{2.5}$	
Dibrugarh (27.3°N, 94.6°E)	Urban	Winter	57.2 ± 32.4	51.9 ± 32.4	Present study
		Pre-monsoon	53.2 ± 27.9	47.8 ± 27.3	
		Monsoon	39.5 ± 19.6	32.0 ± 17.3	
		Post-monsoon	45.0 ± 24.3	37.3 ± 21.3	
Trivundrum (8.55°N, 76.9°E)	Coastal	Winter	59.5	54.1	Pillai et al. (2002)
		Pre-monsoon	51.7	45.2	
		Monsoon	34.9	28.1	
		Post-monsoon	49.8	39.7	
New Delhi (28.6°N, 77.°E)	Urban	Monsoon	∼45–∼196	∼25–∼110	Tiwari et al., 2012
		Winter	∼150–∼1500	∼80–900	
IGP (21.75°-31.0°N, 74.25°-91.5°E)	Urban	Winter		80–100	Di Girolamo et al. (2004)
Hyderabad (17.48°N, 78.4° E)	Urban	Winter	∼30–55	∼22–38	Latha and Badarinath (2005)
		Pre-monsoon	∼15–48	∼8–38	
		Monsoon	∼8–25	∼6–23	
		Post-monsoon	∼32–35	∼30–32	
Ahmadabad (23.03°N, 72.55°E)	Urban	Winter	106	–	Ganguly et al. (2006)
		Pre-monsoon	–	–	
		Monsoon	40	–	
		Post-monsoon	–	–	
Kolkata (22.56° N, 88.36° E)	Urban	Winter	304	179	Das et al. (2006)
Pune (18.72°N, 73.85°E)	Urban	Winter	90	69	Kumar and Joseph (2006)
Chennai (13.1°N, 80.29°E)	Urban	Winter	77–228	36–148	Bathmanabhan et al. (2010)
		Pre-monsoon	29–171	14–94	
		Monsoon	–	–	
		Post-monsoon	147–259	61–126	
Mumbai (18.96°N, 72.83°E)	Urban	Annual	140–231	–	Gupta et al. (2012)
Patiala (Sidhuwal) (30.33°N, 76.46°E)	Rural	Winter	105 ± 4.5	64 ± 3.5	Awasthi et al. (2011)
		Pre-monsoon	–	–	
		Monsoon	86 ± 2.1	48 ± 1.1	
		Post-monsoon	180.5 ± 30.4	123.5 ± 33.2	
Anantapur (14.7°N, 77.6°E)	Semi-urban	Winter	22.07	21.29	Balakrishnaiah et al. (2011)
		Pre-monsoon	18.53	16.34	
		Monsoon	16.46	14.47	
		Post-monsoon	17.76	15.97	

annual variation of the PM concentrations show that the concentration level gradually increased from 2007 to 2010 and decreased thereafter. This is consistent with the fire counts averaged over NE (22°N–30°N, 88°E –98°E) from the moderate resolution imaging spectroradiometer (MODIS) Terra and Aqua satellites (Fig. 3(b)). The gridded MODIS active fire products are generated from MODIS CMG 0.5° products (Giglio et al., 2003) at 1° spatial resolution for time period of one calendar month. The Terra and Aqua satellites crosses the equator (hence the study region) in the forenoon (1030 LT) and afternoon (1330 LT) hours respectively. The fire counts recorded by both the satellites show similar seasonal and annual variation though Aqua counts are higher compared to that of Terra. The difference in the measurements by Terra and Aqua may be attributed to the timing of the satellites passes over the region. Due to gradual decrease of humidity towards noon the biomass burning activity peaks up during mid day and afternoon hours corresponding to the passage of the Aqua satellites.

In general a higher rainfall results in higher aerosol deposition rate. Subsequently less rainfall together with continued generation of PM with its longer lifetime resulted in a steady increase in average PM level throughout the dry months November to February. The observed maximum concentrations of PM_{10} and $PM_{2.5}$ in the year winter 2009–2010 may be associated with lowest annual total rainfall (∼1705 mm) among all the years of observation as well as the drought during winter season with no rainfall in January and only 1 mm and 4 mm of rainfall in December and February respectively (Fig. 3(c)). Reverse is the case in winter 2010–2011 with lower PM concentrations and higher annual rainfall of ∼2587 mm in the year 2010. The decreasing trend in PM concentrations may also be associated with increasing rainfall trend during the last decade particularly over the present study location in spite of overall decreasing rainfall trend in NE India. Similar decreasing trend in BC over the location has also been observed (Fig. 4) for the period June 2008–March 2012. The lowest BC concentration in winter 2011–2012 is associated with observed lowest PM concentrations. The continued decrease in BC over the location may be attributed to reduction in contribution from human activities more precisely the vehicular and household emissions and biomass burning activities. Because with rapid development of life style and adherence to latest emission norms in vehicles and by industries BC together with other species has decreased progressively. Decreasing trend in BC concentration has been reported earlier by Moorthy (2010) over Trivandrum.

3.2. Microphysical and optical parameters of particulate matter

The effective radius, a parameter strongly dependent on the size distribution is significant for characterizing the optical properties of a poly dispersive aerosol system and for ARF calculations (Hansen and Travis, 1974). The effective radius, R_{eff} and mass mean radius, R_m estimated for all daily mean QCM measurements show similar annual variability (Fig. 5). The R_{eff} and R_m start to increase gradually from their lowest value in January (∼0.07 ± 0.01 μm and ∼0.59 ± 0.12 μm respectively) and reach a broad peak during July–September with maximum value of R_{eff} (0.15 ± 0.05 μm) in August and R_m (1.39 ± 0.35 μm) in July. In comparison the R_{eff} at Trivandrum (∼0.26 μm: Beegum et al., 2009) and Anantapur (∼0.45 μm: Reddy et al., 2007) are higher due to possible influence of coarse sea salt aerosols and presence of large mineral soil or dust aerosols respectively.

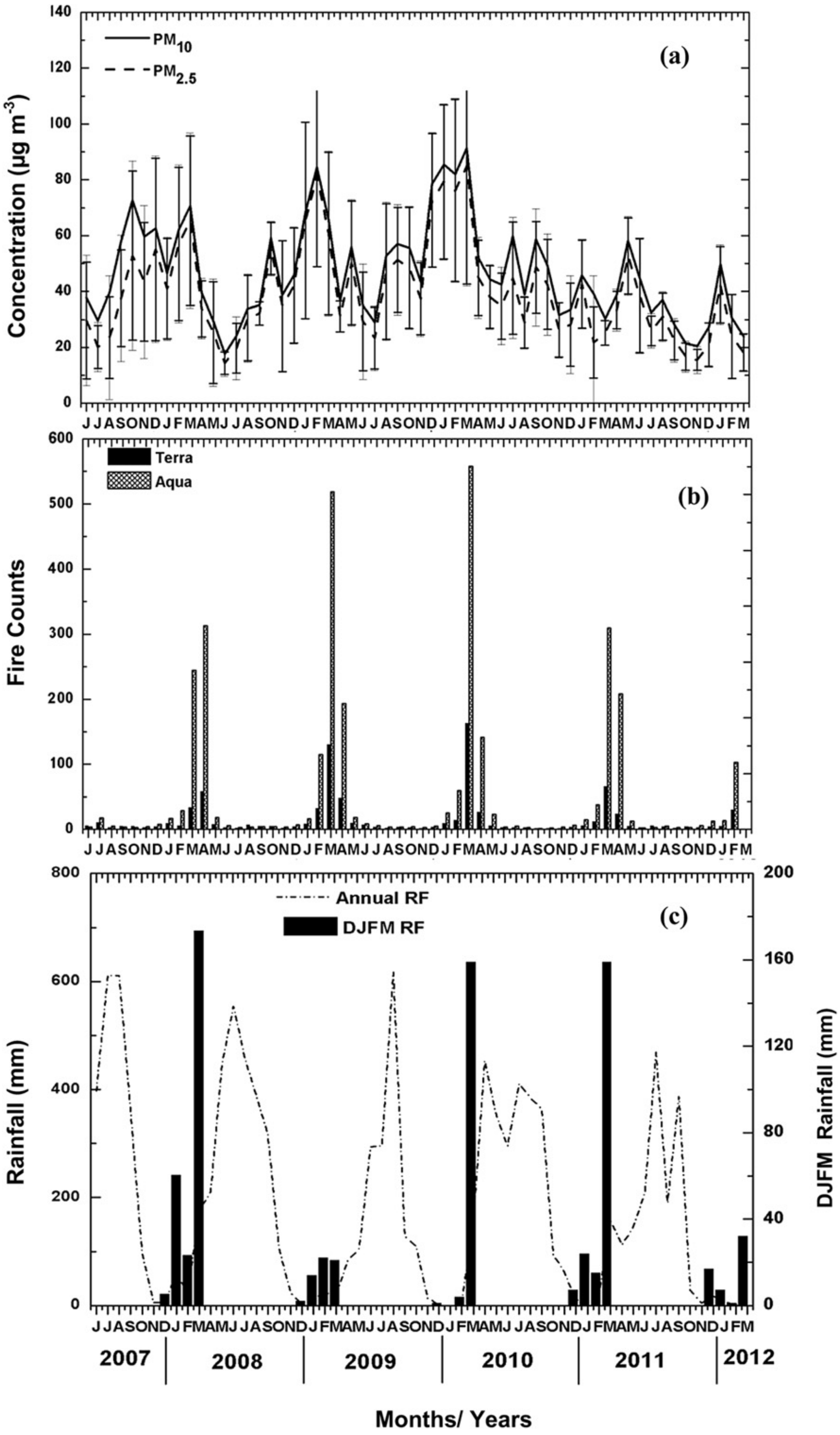

Fig. 3. (a) Time series of monthly mean PM_{10} (solid line) and $PM_{2.5}$ (dashed dot line) (the vertical bars are the standard deviations), (b) Fire counts generated from MODIS Terra (filled bar) and Aqua (dense bar) satellites and (c) monthly total rainfall (dashed-dot line) and December, January, February, March (DJFM) rainfall (filled bar).

The size distribution of aerosols is critical for climate impact studies (IPCC, 2001). The number size distributions obtained for each sample are averaged over each month and season and the resulting climatological seasonal number density-size distributions, d$n(r)$/dr are shown in Fig. 6(a). The number-size decreases monotonically towards the larger size particles inferring the abundance of smaller particles near the surface. Due to the limitation in size resolution of the QCM the present values of d$n(r)$/dr do not provide information regarding ultrafine particles (<0.07 μm) and hence there may be a possibility of ultrafine mode below aerodynamic diameter ~0.07 μm. Similar observation has been reported by Nair et al. (2008) over Arabian Sea (AS) from QCM measurements. However, Sinha et al. (2011) were able to derive a bimodal size distribution over BoB using measurements from a 15 channel optical particle counter (GRIMM 1.108) in the size range (particle diameter) 0.3–20 μm.

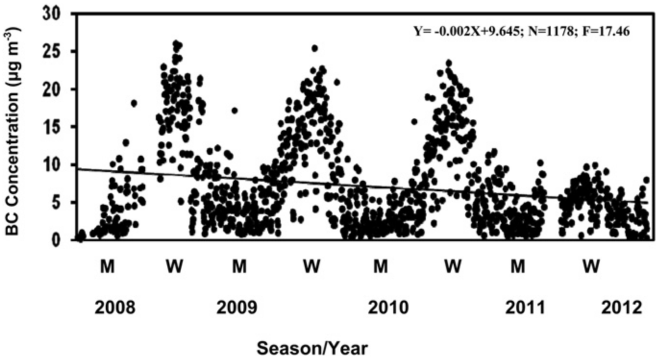

Fig. 4. Time series plot of black carbon mass concentration for the period June 2008–March 2012. M and W denotes monsoon and winter seasons respectively. The solid line is the linear regression through the data points.

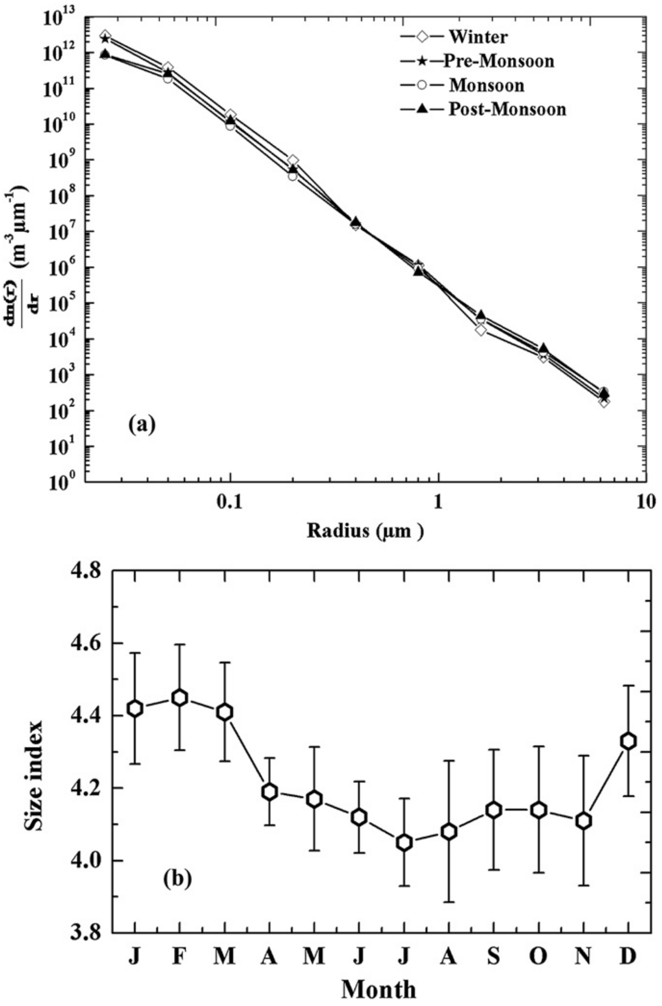

Fig. 6. (a) Seasonal number-size distributions and (b) monthly mean size index of near surface aerosols.

The size index, ν determined from d$n(r)$/dr lies within 4.05 ± 0.12 in July and 4.45 ± 0.15 in February (Fig. 6(b)). The present values of ν lie between those reported over BoB (4.70–5.65) during Winter Integrated Campaign on Aerosols, gases and Radiation Budget (W-ICARB, 2008–2009) by Sinha et al. (2011) and over Arabian Sea, AS (3.8–4.2) during ICARB-2006 by Nair et al. (2008). Sinha et al. (2011) have attributed the higher BoB values to larger accumulation mode fraction while Nair et al. (2008) pointed to large particle heterogeneity over Arabian Sea. The high values of ν obtained over the present location indicate larger fine mode fraction throughout the year. Seasonally, highest value of ν is observed in winter which decreasing gradually through pre-monsoon reaches its lowest level during monsoon. Similar seasonal variation has been observed over Thumba for the period 1998–2000 (Moorthy and Pillai, 2004). The uncertainty in size index follows from those associated with the estimation of d$n(r)$/dr, which is ~20% due to the assumed value of aerosol density (Pillai and Moorthy, 2001).

The extinction of solar radiation due to aerosols present near the surface is evaluated in terms of the extinction coefficient (β_{ext}). It is estimated from the number size distribution (d$n(r)$/dr) assuming a well mixed layer of vertical extent $Z = 1$ km following the Mie

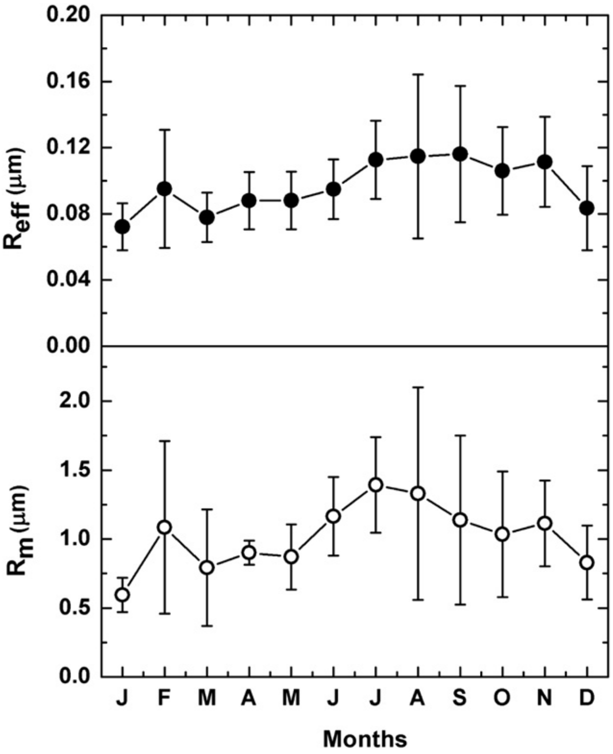

Fig. 5. Variation of monthly mean Effective radius (top panel) and mass mean radius (bottom panel) averaged for the period June 2007–March 2012.

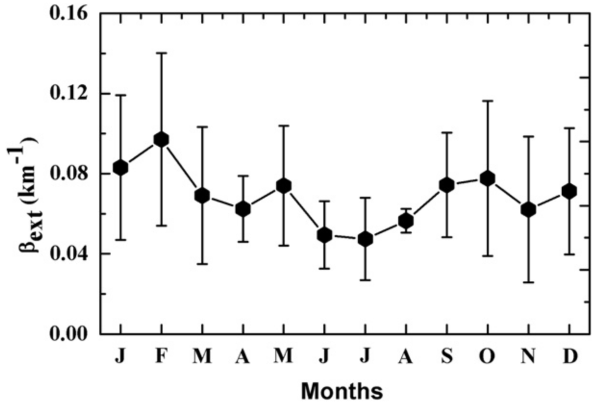

Fig. 7. Variation of monthly averaged near surface aerosol extinction coefficient (β_{ext}) derived from QCM for the period June 2007–March 2012.

scattering theory at wavelength 500 nm using the complex refractive index ($m \sim 1.52{-}0.0066i$) for rural aerosol model of Shettle and Fenn (1979); d'Almeida et al. (1991). The climatological mean annual variation of the β_{ext} thus estimated is presented in Fig. 7 for the period June 2007–March 2012. The β_{ext} peaks in winter (0.07–0.1 km^{-1}) and attains minimum value in monsoon (0.05–0.07 km^{-1}). Nair el al. (2008) have reported the β_{ext} value lying within 0.04–0.1 km^{-1} over Arabian Sea following the same methodology. Gadhavi and Jayaraman (2006) have reported β_{ext} values upto 0.2 km^{-1} within 1 km from the surface in winter from ground based Lidar measurement over Hyderabad. Similarly, Satheesh et al. (2009) have obtained β_{ext} value upto 0.15 km^{-1} over Bhubaneswar (20.23°N, 85.82°E), Trivandrum and Chennai from air-borne Lidar measurements during pre-monsoon, 2006, while Komppula et al. (2010) have reported annual average β_{ext} value of 0.14 km^{-1} at 532 nm over Gual Pahari (28.43°N, 77.15°E), near New Delhi from Raman Lidar measurements. Ganguly et al. (2006) over Ahmedabad and Komppula et al. (2010) over Gual Pahari have observed very high values of extinction coefficient from ground based Lidar measurements within few hundred metres from the surface during winter (dry) season.

3.3. Contribution of BC to PM$_{10}$ and PM$_{2.5}$

BC being a major constituent of PM in the atmosphere, in order to examine its contributions to PM concentrations, fractions of BC over PM$_{10}$ and PM$_{2.5}$ are estimated. It has been observed that the percentage contribution of BC to PM$_{10}$ varies from 7.6% in post-monsoon to 4.7% in monsoon, whereas those for winter and pre-monsoon seasons are 7.5% and 5.1% respectively. On the other hand BC fraction in PM$_{2.5}$ varies from 9.2% in post-monsoon to 5.6% in pre-monsoon and those for winter and monsoon seasons are 8.3% and 5.7% respectively. The lowest BC fraction in PM$_{2.5}$ in pre-monsoon season can be attributed to the abundance of larger size particulates compared to monsoon season. Apart from vehicular emissions, indoor/outdoor burnings and transportation from nearby oil wells as well as from distant places contributes to BC over Dibrugarh. To identify whether the BC or organic carbon (OC) are dominant and hence to delineate the sources of absorbing aerosols, the wavelength variation of absorption coefficient is estimated using a power law relationship of the form (Kirchstetter et al., 2004)

$$\beta_{abs}(\lambda) = K\lambda^{-\alpha_{abs}} \qquad (4)$$

where K and α_{abs} are the absorption Ångström coefficients and α_{abs} is a measure of spectral dependence of aerosol absorption. Fig. 8 shows that the monthly mean α_{abs} values lies in the range ~1.1–1.5 for the study period. These values reveal the stronger spectral dependence of α_{abs} over the location. It has been reported that the aerosols produced from the biomass burning containing higher amount of OC exhibit stronger wavelength dependence ($\alpha_{abs} \geq 2$) in the absorption while those produced from fossil fuel burning

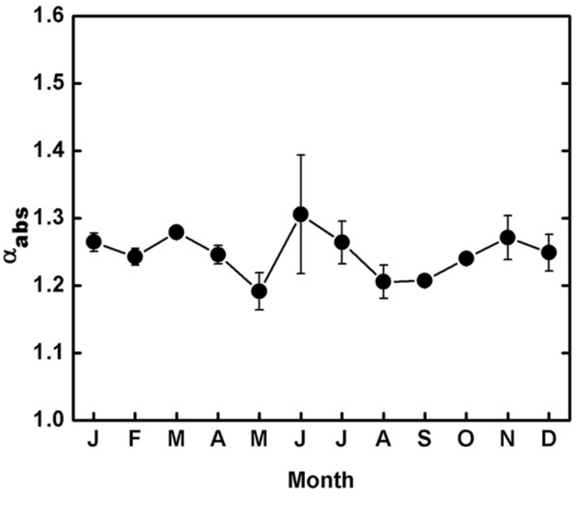

Fig. 8. Monthly averaged absorption Ångström exponent, α_{abs} for the period June 2008–March 2012.

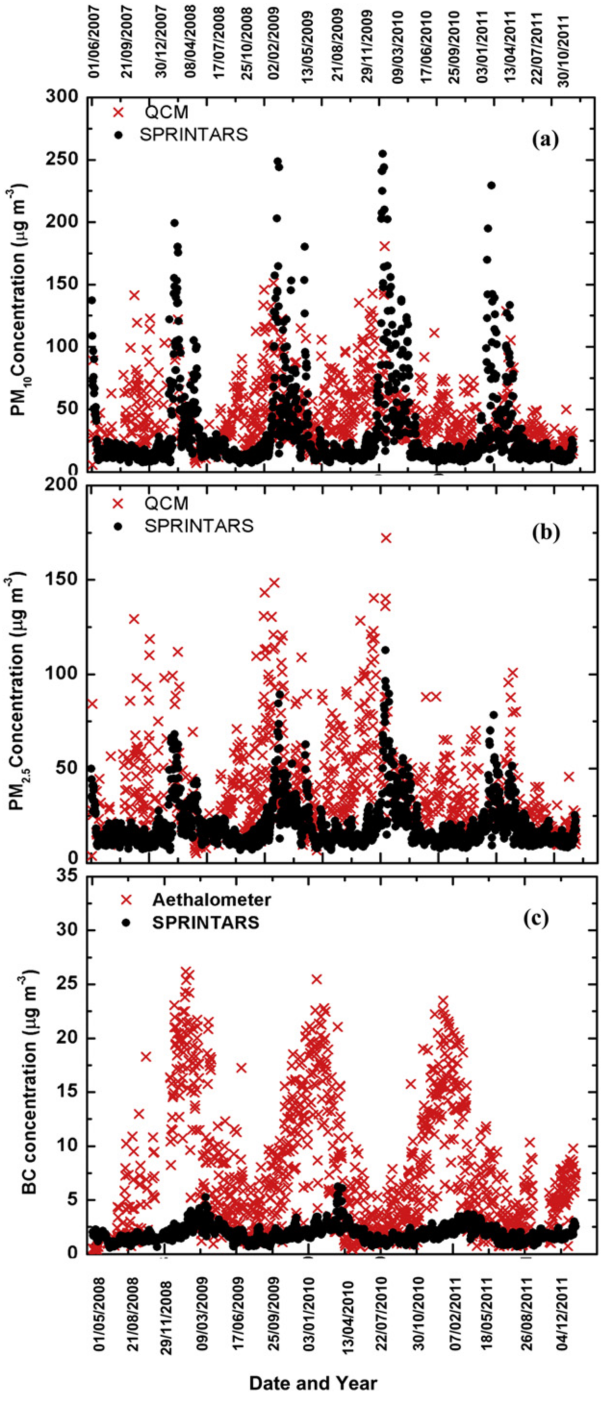

Fig. 9. Time series plot of measured and simulated concentrations of (a) PM$_{10}$, and (b) PM$_{2.5}$ for the period June 2007–December 2011 and (c) BC for the period June 2008–December 2011.

containing higher amount of BC such as motor vehicle exhausts etc. show a weaker dependence ($\alpha_{abs} \leq 1$) (Kirchstetter et al., 2004). Thus higher α_{abs} (≥ 2) is indication of higher OC/BC ratio, while low $\alpha_{abs} \leq 1$ represents high BC/OC, typical for the fossil-fuel combustion. This observation, hence, suggests the stronger presence of absorbing aerosols originating from biomass burning than those originating from fossil fuel burning. The OC concentrations are dominated by secondary organic aerosols, which besides from biomass burning and anthropogenic sources may also result from the large biogenic volatile organic carbon emissions from the tea gardens and vegetation surrounding the study location.

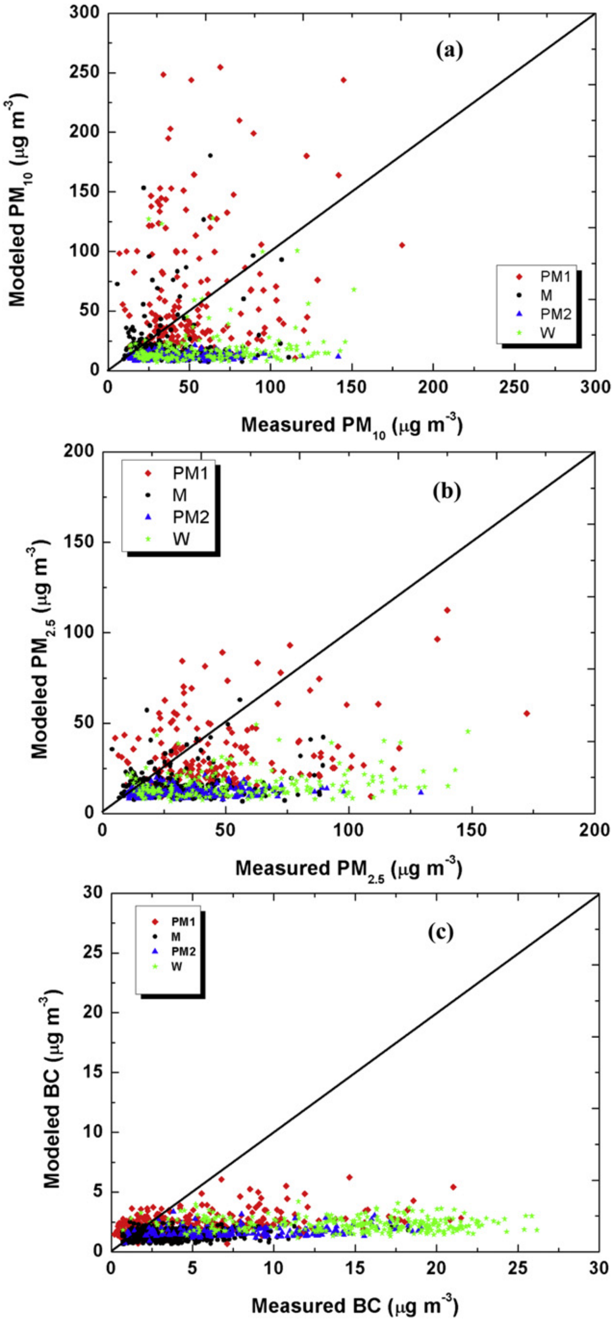

Fig. 10. Scatter plot between measured and modelled concentrations of (a) PM_{10}, (b) $PM_{2.5}$ and (c) BC for four seasons: pre-monsoon (PM1), monsoon (M), post-monsoon (PM2) and winter (W) for the period June 2007–December 2011 for PMs and June 2008–December 2011 for BC.

3.4. *Inter-comparison of measured PM and BC concentrations with SPRINTARS simulation*

Intercomparison of the model simulation with measured data provides valuable information regarding the validity of the model estimates. Fig. 9(a–c) show the time series of the measured and model simulated PM and BC concentrations. It is observed that the measured PM and BC concentrations attain peak in winter while model concentrations are highest in the pre-monsoon season. The PM_{10}, $PM_{2.5}$ and BC are further compared with SPRINTARS simulations by scatter plot among them (Fig. 10(a–c)). It is seen that majority of the data points are weighted in favour of the measured PM concentrations indicating underestimation by the model. Comparison of the PM_{10} seasonal concentrations (Table 2) clearly shows that the model underestimates by 38%, 69% and 64% in monsoon, post-monsoon and winter respectively while it overestimates by 36% in pre-monsoon season. For $PM_{2.5}$ concentrations the model underestimates in all seasons. The underestimation varies from a minimum of 24% in pre-monsoon to a maximum of 69% in winter. Similarly measured BC concentration is higher than the model estimates except during pre-monsoon season. It may also be noted that the underestimation is large compared to that in case of PMs and nearly all the points are weighted towards the measured data. Koch et al. (2009), who compared BC simulations from about 20 global models have shown that SPRINTARS successfully captures the large annual mean BC concentrations in Southeast Asia and overestimates it in other regions of the Globe. Goto et al. (2011a) have also reported similar underestimation by model simulation of BC by a factor of 20 over Hyderabad. Goto et al. (2011b) have also ascertained large impact of different BC emission inventories on ARF. The seasonal discrepancies observed in the present study might have arisen due to the topography of the location where aerosols from distant sources in addition to local emissions are trapped between the mountains and inadequate emission inventory for this climate zone. Other possible reasons might be associated with the assumed mixing state of BC and other particles, which does not represent that in the real atmosphere and coarse grid size (~2.8° × 2.8°) that does not exactly match with surface point observations (Goto et al., 2011a). According to Koch et al. (2009) as validation exercises of global models over India have not been performed due to lack of sufficient measurements, these problems are expected. Further, the complex aerosol

Table 2
Seasonal mean vales of measured and model estimates for PM_{10}, $PM_{2.5}$ and BC.

Seasons	PM_{10} ($\mu g\ m^{-3}$)		$PM_{2.5}$ ($\mu g\ m^{-3}$)		BC ($\mu g\ m^{-3}$)	
	QCM	SPRINTARS	QCM	SPRINTARS	Aethalometer	SPRINTARS
Winter	56.6 ± 32.1	20.1 ± 18.0	52.5 ± 32.4	16.6 ± 7.2	13.2 ± 6.2	2.3 ± 0.6
Pre-monsoon	50.1 ± 28.9	68.7 ± 49.9	45.5 ± 28.1	34.5 ± 16.7	5.3 ± 4.1	2.4 ± 0.8
Monsoon	35.7 ± 18.5	21.7 ± 18.9	30.2 ± 16.7	16.8 ± 7.4	3.5 ± 2.6	1.3 ± 0.4
Post-monsoon	41.5 ± 22.4	12.8 ± 2.8	35.2 ± 20.2	12.5 ± 2.8	8.3 ± 4.4	1.7 ± 0.4

environment over India makes comparison of models with measurements difficult.

4. Conclusions

The long term climatology of PM_{10} and $PM_{2.5}$ concentrations over Dibrugarh have been studied and the contribution of BC to PM_{10} and $PM_{2.5}$ are examined. The measured concentrations are compared with SPRINTARS model simulations. The following conclusions are drawn.

(i) Fine fraction $PM_{2.5}$ is the principal contributor to the PM_{10} concentration. Both PM_{10} and $PM_{2.5}$ exhibit similar seasonal variability with maximum in winter and minimum in monsoon. The annual maximum is observed in late winter or early summer every year. Highest PM concentrations are positively correlated with fire counts over NE India and negatively correlated with rainfall over the location.

(ii) A slow decreasing trend in the PMs and BC concentrations has been observed during the study period.

(iii) The microphysical and optical parameters of near surface aerosols reveal the dominance of fine aerosols contributing to extinction of light.

(iv) Intercomparison of measured PM and BC concentrations with SPRINTARS model simulations shows that the model underestimates the measured concentrations of PMs and BC except during pre-monsoon. The model does not reproduce the observed seasonal variations either in PMs or BC which may be due to the topography of the location and inadequate emission inventory for the climate zone.

Acknowledgements

This work was carried out as part of the ISRO GBP ARFI project. Binita Pathak and Jhuma Biswas are indebted to the ISRO for providing them Associateship/fellowship under the ARFI project. The authors are grateful to the Project Director K. Krishna Moorthy and S. Suresh Babu for their constant encouragement and support. The fire count data are downloaded from the ftp://neespi.gsfc.nasa.gov/data/s4pa/Fire. The Authors are grateful to the anonymous referees for their comments and suggestions towards the improvement of this work.

References

Arnott, W.P., Hamasha, K., Moosmuller, H., Sheridan, P.J., Ogren, J.A., 2005. Towards aerosol light-absorption measurements with a 7-wavelength aethalometer: evaluation with a photoacoustic instrument and 3-wavelength Nephelometer. Aerosol Science and Technology 39 (1), 17–29. http://dx.doi.org/10.1080/027868290901972.

Awasthi, A., Agarwal, R., Mittal, S.K., Singh, N., Singh, K., Gupta, P.K., 2011. Study of size and mass distribution of particulate matter due to crop residue burning with seasonal variation in rural area of Punjab, India. Journal of Environmental Monitoring 13, 1073–1081.

Babu, S.S., Moorthy, K.K., Satheesh, S.K., 2004. Aerosol black carbon over Arabian Sea during intermonsoon season and summer monsoon season. Geophysical Research Letter 31, L06104. http://dx.doi.org/10.1029/2003GL018716.

Balakrishnaiah, G., et al., 2011. Characterization of PM, PM_{10} and $PM_{2.5}$ mass concentrations at a tropical semi-arid station in Anantapur, India. Indian Journal of Radio & Space Physics 40, 95–104.

Bathmanabhan, S., Nagendra, S., Madanayak, S., 2010. Analysis and interpretation of particulate matter – PM_{10}, $PM_{2.5}$ and PM_1 emissions from the heterogeneous traffic near an urban roadway. Atmospheric Pollution Research 1, 184–194.

Beegum, N., Moorthy, K.K., Babu, S.S., 2009. Aerosol microphysics over a tropical coastal station inferred from the spectral dependence of Angstrom wavelength exponent and inversion of spectral aerosol optical depths. Journal of Atmospheric and Solar-Terrestrial Physics 71, 1846–1857.

d'Almeida, G.A., Koepke, P., Shettle, E.P., 1991. Atmospheric Aerosols-global Climatology and Radiative Characteristics. A. Deepak, Hampton, VA.

Das, M., Maiti, S.K., Mukhopadhyay, U., 2006. Distribution of $PM_{2.5}$ and $PM_{10-2.5}$ in PM_{10} fraction in ambient air due to vehicular pollution in Kolkata megacity. Environtal Monitoring Assessment 122, 111–123. http://dx.doi.org/10.1007/s10661-005-9168-3.

Di Girolamo, L., Bond, T.C., Bramer, D., Diner, D.J., Fettinger, F., Kahn, R.A., et al., 2004. Analysis of Multi-Angle Imaging Spectroradiometer (MISR) aerosol optical depths over greater India during winter 2001–2004. Geophysical Research Letter 31, L23115. http://dx.doi.org/10.1029/2004GL021273.

Forster, P., et al., 2007. Changes in atmospheric constituents and in radiative forcing. In: Solomon, S., et al. (Eds.), Climate Change 2007: The Physical Science Basis. Contribution of Working Group I to the Fourth Assessment Report of the Intergovernmental Panel on Climate Change. Cambridge University Press, Cambridge, United Kingdom and New York, NY, USA.

Gadhavi, H., Jayaraman, A., 2006. Airborne lidar study of the vertical distribution of aerosols over Hyderabad, an urban site in central India, and its implication for radiative forcing calculations. Annales Geophysicae 24, 2461–2470.

Ganguly, D., Jayaraman, A., Gadhavi, H., 2006. Physical and optical properties of aerosols over an urban location in western India: seasonal variabilities. Journal of Geophysical Research 111, D24206. http://dx.doi.org/10.1029/2006JD007392.

Giglio, L., Descloitres, J., Justice, C.O., Kaufman, Y.J., 2003. An enhanced contextual fire detection algorithm for MODIS. Remote Sensing of Environment 87 (2–3), 273–282.

Gogoi, M.M., Bhuyan, P.K., Moorthy, K.K., 2008. Estimation of the effect of long range transport on seasonal variation of aerosols over north eastern India. Annales Geophysicae 26, 1365–1377.

Gogoi, M.M., Bhuyan, P.K., Moorthy, K.K., 2009a. Climatology of columnar aerosol properties and the influence of synoptic conditions: first-time results from the north-eastern region of India. Journal of Geophysical Research 114, D08202. http://dx.doi.org/10.1029/2008JD010765.

Gogoi, M.M., Moorthy, K.K., Babu, S.S., Bhuyan, P.K., 2009b. An investigation of aerosol size distribution properties at Dibrugarh: north-eastern India. Terrestrial Atmospheric Oceanic Sciences 20 (3). http://dx.doi.org/10.3319/TAO.2008.06.11.01 (A).

Gogoi, M.M., Pathak, B., Moorthy, K.K., Bhuyan, P.K., Babu, S.S., Bhuyan, K., Kalita, G., 2011. Multi-year investigations of near surface and columnar aerosols over Dibrugarh, North-Eastern location of India: heterogeneity in source impacts. Atmospheric Environment. http://dx.doi.org/10.1016/j.atmos env.2010.12.056.

Goto, D., Badarinath, K.V.S., Takemura, T., Nakajima, T., 2011a. Simulation of aerosol optical properties over a tropical urban site in India using a global model and its comparison with ground Measurements. Annales Geophysicae 29, 955–963.

Goto, D., Takemura, T., Nakajima, T., Badarinath, K.V.S., 2011b. Global aerosol model-derived black carbon concentration and single scattering albedo over Indian region and its comparison with ground observations. Atmospheric Environment 45, 3277–3285.

Gupta, I., Salunkhe, A., Kumar, R., 2012. Source apportionment of PM_{10} by positive matrix factorization in urban area of Mumbai, India. The Scientific World Journal 2012, 585791. http://dx.doi.org/10.1100/2012/585791.

Hansen, J.E., Travis, L.D., 1974. Light scattering in planetary atmosphere. Space Science Reviews 16, 527–610.

Hansen, A.D.A., Rosen, H., Novakov, T., 1984. The aethalometer – an instrument for the real-time measurement of optical absorption by aerosol particles. Science of Total Environment 36, 191–196.

IPCC, 2001. Climate Change 2001, Working Group I: the Scientific Basis, Chapter 5: Aerosols, Their Direct and Indirect Effects, pp. 291–348.

Kalita, G., Bhuyan, P.K., 2011. Spatial heterogeneity in tropospheric ozone over the Indian subcontinent: long-term climatology and possible association with natural and anthropogenic activities. Advances in Meteorology, 924516. http://dx.doi.org/10.1155/2011/924516.

Kirchstetter, T.W., Novakov, T., Hobbs, P.V., 2004. Evidence that the spectral dependence of light absorption by aerosols is affected by organic carbon. Journal of Geophysical Research 109, D21208. http://dx.doi.org/10.1029/2004JD004999.

Koch, D., et al., 2009. Evaluation of black carbon estimations in global aerosol models. Atmospheric Chemistry and Physics 9, 9001–9026.

Komppula, M., et al., 2010. One year of Raman-lidar measurements in Gual Pahari EUCAARI site close to New Delhi in India: seasonal characteristics of the aerosol vertical structure. Atmospheric Chemistry and Physics Discussion 10, 31123–31151.

Kumar, R., Joseph, A.E., 2006. Air pollution concentrations of $PM_{2.5}$, PM_{10} and NO_2 at ambient and Kerbsite and their correlation in metro city—Mumbai. Environmental Monitoring Assessment 119 (1–3), 191–199.

Latha, K.M., Badarinath, K.V., 2005. Seasonal variations of PM_{10} and $PM_{2.5}$ particles loading over tropical urban environment. International Journal of Environmental and Health Research 15 (1), 63–68.

Moorthy, K.K., Pillai, P.S., 2004. Aerosol Climatology and Effects-II, Characterization of Near Surface Aerosols at Thumba. ISRO-GBP Scientific Report.

Moorthy, K.K., Babu, S.S., Satheesh, S.K., 2005. Aerosol characteristics and radiative impacts over the Arabian Sea during inter-monsoon season: results from the ARMEX field campaign. Journal of Atmospheric Science 62, 192–206. http://dx.doi.org/10.1175/JAS-3378.1.

Moorthy, K.K., Babu, S.S., Satheesh, S.K., 2007. Temporal heterogeneity in aerosol characteristics and the resulting radiative impact at a tropical coastal station-part 1: microphysical and optical properties. Annales Geophysicae 25, 2293–2308.

Moorthy, K.K., Satheesh, S.K., Babu, S.S., Dutt, C.B.S., 2008. Integrated Campaign for Aerosols, Gases and Radiation Budget (ICARB): an overview. Journal of Earth System Science 117 (S1), 243–262.

Moorthy, K.K., 2010. ARFI & ICARB Scientific Progress Report-2010, ISRO Geosphere Biosphere Program, pp. xvi.

Nair, V.S., et al., 2007. Wintertime aerosol characteristics over the Indo-Gangetic Plain (IGP): impacts of local boundary layer processes and long-range transport. Journal of Geophysical Research 112, D13205. http://dx.doi.org/10.1029/2006JD008099.

Nair, V.S., Moorthy, K.K., Babu, S.S., Narasimhulu, K., Reddy, L.S.S., Reddy, R.R., Gopal, K.R., Sreekanth, V., Madhavan, B.L., Niranjan, K., 2008. Size segregated aerosol mass concentration measurements over the Arabian Sea during ICARB. Journal Earth System Science 117, 315–323.

Pant, P., Hegde, P., Dumka, U.C., Saha, A., Srivastava, M.K., Sagar, R., 2006. Aerosol characteristics at a high-altitude location during ISRO-GBP Land Campaign-II. Current Science 91 (8), 1053–1061.

Pathak, B., Kalita, G., Bhuyan, K., Bhuyan, P.K., Moorthy, K.K., 2010. Aerosol temporal characteristics and its impact on shortwave radiative forcing at a location in the northeast of India. Journal of Geophysical Research 115, D19204. http://dx.doi.org/10.1029/2009JD013462.

Pathak, B., Bhuyan, P.K., Gogoi, M.M., Bhuyan, K., 2012. Seasonal heterogeneity in aerosol types over Dibrugarh-North-Eastern India. Atmospheric Environment. http://dx.doi.org/10.1016/j.atmosenv.2011.10.061.

Pillai, P.S., Moorthy, K.K., 2001. Aerosol mass-size distributions at a tropical coastal station. Response to Mesoscale and Synoptic Processes. Atmospheric Environment 35, 4099–4112.

Pillai, P.S., Babu, S.S., Moorthy, K.K., 2002. A study of PM, PM_{10} and $PM_{2.5}$ concentration at a tropical coastal station. Atmospheric Research 61, 149–167.

Reddy, R.R., et al., 2007. Aerosol size distribution variation in Anantapur (14.62°N, 77.65°E) semi arid zone and its impact on aerosol effective radius. Aerosol and Air Quality Research 7 (4), 550–562.

Satheesh, et al., 2009. Vertical structure and horizontal gradients of aerosol extinction coefficients over coastal India inferred from airborne lidar measurements during the Integrated Campaign for Aerosol, Gases and Radiation Budget (ICARB) field campaign. Geophysical Research Letter 114, D05204. http://dx.doi.org/10.1029/2008JD011033.

Shettle, E.P., Fenn, R.W., 1979. Models for the Aerosols of the Lower Atmosphere and the Effects of Humidity Variations on Their Optical Properties. AFGL-TR-79–0214, Environmental Research Paper No. 676. Air Force Geophysics Laboratory, MA, USA, 26 pp.

Sinha, P.R., et al., 2011. Spatial heterogeneities in aerosol size distribution over Bay of Bengal during Winter-ICARB Experiment. Atmospheric Environment 45, 4695–4706.

Song, C.K., Ho, C.H., Park, R.J., Choi, Y.S., Kim, J., Gong, D.Y., Lee, Y.B., 2009. Spatial and seasonal variations of surface PM_{10} concentration and MODIS aerosol optical depth over China, Asia-Pacific. Journal of Atmospheric Science 45 (1), 33–43.

Takemura, T., Egashira, M., Matsuzawa, K., Ichijo, H., O'ishi, R., Abe-Ouchi, A., 2009. A simulation of the global distribution and radiative forcing of soil dust aerosols at the Last Glacial Maximum. Atmospheric Chemistry and Physics 9, 3061–3073.

Tiwari, S., Chate, D.M., Pragya, P., Ali, K., Bisht, D.S., 2012. Variations in Mass of the PM_{10}, $PM_{2.5}$ and PM_1 during the Monsoon and the winter at New Delhi. Aerosol and Air Quality Research 12, 20–29.

Weingartner, E., Saathoff, H., Schnaiter, M., Strit, N., Bitnar, B., Baltensperger, U., 2003. Absorption of light by soot particles: determination of the absorption coefficient by means of Aethalometers. Journal of Aerosol Science 34, 1445–1463.

Ye, B.X., et al., 2003. Concentration and chemical composition of $PM_{2.5}$ in Shanghai for 1-year period. Atmospheric Environment 37, 499–510.